Role of Aromatic Stacking Interactions in the Modulation of the Two-Electron Reduction Potentials of Flavin and Substrate/Product in *Megasphaera elsdenii* Short-Chain Acyl-Coenzyme A Dehydrogenase[†]

Jackson D. Pellett,[‡] Donald F. Becker,[‡,§] Amy K. Saenger,[‡] James A. Fuchs,[||] and Marian T. Stankovich*[,‡]

Department of Chemistry, University of Minnesota, 207 Pleasant Street SE, Kolthoff and Smith Halls, Minneapolis, Minnesota 55455, and Department of Biochemistry, University of Minnesota, 1479 Gortner Avenue, Gortner Laboratory, St. Paul, Minnesota 55108-1022

Received January 31, 2001; Revised Manuscript Received May 2, 2001

ABSTRACT: The effects of aromatic stacking interactions on the stabilization of reduced flavin adenine dinucleotide (FAD) and substrate/product have been investigated in short-chain acyl-coenzyme A dehydrogenase (SCAD) from *Megasphaera elsdenii.* Mutations were made at the aromatic residues Phe160 and Tyr366, which flank either face of the noncovalently bound flavin cofactor. The electrochemical properties of the mutants were then measured in the presence and absence of a butyryl-CoA/crotonyl-CoA mixture. Results from these redox studies suggest that the phenylalanine and tyrosine both engage in favorable $\pi-\sigma$ interactions with the isoalloxazine ring of the flavin to help stabilize formation of the anionic flavin hydroquinone. Disruption of these interactions by replacing either residue with a leucine (F160L and Y366L) causes the midpoint potential for the oxidized/hydroquinone couple ($E_{ox/hq}$) to shift negative by 44−54 mV. The $E_{ox/hq}$ value was also found to decrease when aromatic residues containing electron-donating heteroatoms were introduced at the 160 position. Potential shifts of −32 and −43 mV for the F160Y and F160W mutants, respectively, are attributed to increased $\pi-\pi$ repulsive interactions between the ring systems. This study also provides evidence for thermodynamic regulation of the substrate/product couple in the active site of SCAD. Binding to the wild-type enzyme caused the midpoint potential for the butyryl-CoA/crotonyl-CoA couple ($E_{BCoA/CCoA}$) to shift 14 mV negative, stabilizing the oxidized product. Formation of product was found to be even more favorable in complexes with the F160Y and F160W mutants, suggesting that the electrostatic environment around the flavin plays a role in substrate/product activation.

Acyl-coenzyme A dehydrogenases (ACDs)[1] are flavoproteins that catalyze the interconversion of *trans*-2-enoyl-CoA and saturated acyl-CoA thioesters in mammalian and bacterial systems (*1*). This reaction occurs in mammalian mitochondria as the first step in the β-oxidation cycle (*2*, *3*). The mammalian ACDs are responsible for transferring two electrons from a fatty acyl-CoA substrate to a noncovalently bound flavin adenine dinucleotide (FAD) cofactor. These electrons are then passed one at a time to an electron-transferring flavoprotein (ETF) and ultimately to the respiratory electron-transport chain. In contrast, the *Megasphaera elsdenii* short-chain acyl-CoA dehydrogenase (SCAD) functions primarily as an enoyl-CoA reductase in its physiological environment, transferring electrons from ETF to short-chain (C_3-C_6) *trans*-2-enoyl-CoA thioesters (*4*). This reaction provides the anaerobic bacterium with a means of disposing excess reducing equivalents generated during the fermentation of glucose, fructose, lactate, and other simple carbon compounds (*5*, *6*). However, in vitro, *M. elsdenii* SCAD behaves like its mammalian counterpart and oxidizes fatty acids quite efficiently.

The kinetics and thermodynamics of electron-transferring processes in ACDs, as well as all flavoproteins, are regulated by interactions between the isoalloxazine ring of the flavin and the surrounding protein environment. These interactions include π-stacking (*7*−*9*), hydrogen bonding (*10*−*12*), dipole/multidipole (*13*), and solvent interactions with the conjugated flavin ring system. In ACDs, these interactions are particularly important for stabilizing negative charge that develops in the N(1)−C(2)═O locus of the reduced FAD (hydroquinone) cofactor. The reduced FAD tends to bind 300−5000-fold tighter than oxidized FAD to ACDs, and as a result, the midpoint potentials of oxidized/hydroquinone couples ($E_{ox/hq}$) are 105−144 mV (*14*−*16*) more positive than in the free solution (−219 mV at pH 7) (*17*).

[†] This work was supported by a grant from the National Institutes of Health (GM29344) to M.T.S.

* To whom correspondence should be addressed at the Department of Chemistry, University of Minnesota, 207 Pleasant St. SE, Minneapolis, MN 55455. Phone: (612) 624-1019. Fax: (612) 626-7541. E-mail: stankovi@chem.umn.edu.

[‡] Department of Chemistry.

[§] Present address: Department of Chemistry, University of Missouri−St. Louis, St. Louis, MO 63121.

[||] Department of Biochemistry.

[1] Abbreviations: CoA, coenzyme A; FAD, flavin adenine dinucleotide; ACD, acyl-coenzyme A dehydrogenase; SCAD, short-chain acyl-coenzyme A dehydrogenase; ETF, electron-transferring flavoprotein; BCoA, butyryl-coenzyme A; CCoA, crotonyl-coenzyme A; E_m, general midpoint potential; $\tilde{E}_m$, conditional midpoint potential; $E_{ox/hq}$, midpoint potential for the flavin oxidized/hydroquinone couple; $E_{ox/sq}$, midpoint potential for the flavin oxidized/semiquinone couple; $E_{sq/hq}$, midpoint potential for the flavin semiquinone/hydroquinone couple; $E_{BCoA/CCoA}$, midpoint potential for the butyryl-coenzyme A/crotonyl-coenzyme A couple; SHE, standard hydrogen electrode; SDS, sodium dodecyl sulfate.

10.1021/bi010206s CCC: $20.00
Published on Web 06/02/2001

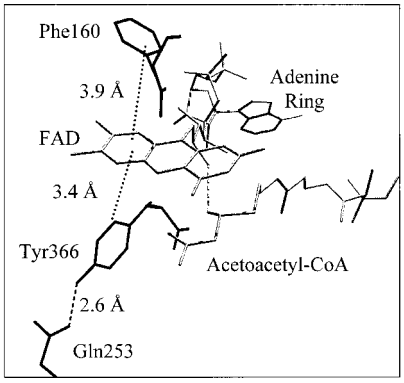

FIGURE 1: Orientation of Phe160 and Tyr366 relative to flavin adenine dinucleotide in *M. elsdenii* short-chain acyl-CoA dehydrogenase. The figure was created using X-ray crystal data obtained by Djordjevic et al. (*19*) with acetoacetyl-CoA bound in the enzyme active site. Phe160 is located at the *si*-side of the flavin ring. Tyr366 lies on the *re*-side of the flavin with the phenolic hydroxyl group within hydrogen bonding distance (2.6 Å) of the Gln253 carbonyl oxygen.

M. elsdenii SCAD has been cloned and overexpressed in *Escherichia coli* (*18*), and its three-dimensional structure has been solved at 2.5 Å resolution with acetoacetyl-CoA bound in the enzyme active site (*19*). In addition, the midpoint potentials of the wild-type enzyme and the site-directed mutant E367Q have been established in the absence and presence of several CoA ligands (*15, 16, 19, 20*). Since the structural and redox properties of *M. elsdenii* SCAD have been well-characterized, the enzyme is a good model system for investigating the role of apoprotein−flavin interactions in ACD regulation. The $E_{ox/hq}$ value for *M. elsdenii* SCAD-bound FAD is reported to be between −75 and −79 mV versus SHE (*15, 16, 20*), a significant positive shift from −219 mV. Thus, apoprotein−flavin interactions in SCAD stabilize the two-electron-reduced flavin by ca. 7 kcal mol^{-1}. Substrate/product binding causes the flavin midpoint potential to shift even more positive, to a value (−19 mV) that is remarkably close to the midpoint potential of the free butyryl-CoA/crotonyl-CoA couple (−13 mV) (*20*). The results of subsequent electrochemical and Raman studies indicate that at least some of this 60 mV positive shift is the result of favorable interactions between the electron-rich reduced flavin and an electron-deficient region on crotonyl-CoA (*16, 21*−*23*).

In the present study, the roles of two aromatic residues, Phe160 and Tyr366, in the thermodynamic regulation of *M. elsdenii* SCAD have been investigated. These residues flank either face of the isoalloxazine ring of the flavin (Figure 1), and are likely to be involved in π-stacking interactions with the flavin. Tyr366 is conserved in all straight-chain ACDs and is located in the bottom of the substrate binding pocket (*19, 24*−*26*). The phenolic side chain of this residue is nearly perpendicular with the *re*-face of the flavin and may be held in position through hydrogen bonding interactions with Gln253. Replacement of the equivalent tyrosine in MCAD with a glycine or phenylalanine causes the midpoint potential of MCAD to become 44 and 18 mV more negative, respectively (*27*). These shifts are attributed to increased solvent accessibility of the flavin, but also may reflect changes in aromatic stacking interactions with the flavin. The phenylalanine at position 160, on the other hand, is not conserved throughout the ACD family. In most mammalian ACDs, a tryptophan is found at the analogous position on the *si*-face of the *o*-xylene subnucleus of the isoalloxazine ring. It has been suggested that the bulky indole side chain is important for protection of the reduced ACDs from molecular oxygen and that the residue may also be involved in electron transfer to ETF (*19, 25*).

Phe160 and Tyr366 have been systematically replaced with other residues (leucine, tryptophan, tyrosine, and phenylalanine), and the redox properties of the resulting mutants have been characterized. In an effort to determine how the mutations affect the redox potential shifts caused by substrate/product binding, $E_{ox/hq}$ values were determined for all of the SCAD mutants in the presence of butyryl-CoA/crotonyl-CoA mixtures. Finally, the midpoint potentials of the butyryl-CoA/crotonyl-CoA couple bound to the mutant enzymes were estimated from anaerobic titrations with butyryl-CoA.

MATERIALS AND METHODS

Site-Directed Mutagenesis of Recombinant Wild-Type SCAD. All site-directed mutations were made on a cloned wild-type *M. elsdenii* SCAD gene (*16, 18*) using the Kunkel method (*28*). Mutagenic primers (antisense oligonucleotides) were as follows: F160L, 5′-TTG GTG ATG AGG ATC TTG-3′; F160Y, 5′-TTG GTG ATG TAG ATC TTG-3′; F160W, 5′-CGT TGG TGA TCC AGA TCT TGG-3′; Y366L, 5′-GTT CGT GCC TTC CAG GAT CTG AGT AAT-3′; Y366F, 5′-GTG CCT TCG AAG ATC TGA-3′; Y366W, 5′-TCG TGC CTT CCC AGA TCT GAG-3′. The underlined nucleotides indicate those nucleotides that differ from wild-type. The 1.6 kb fragments containing mutations for F160L, Y366L, and Y366F SCAD were each subcloned into the pUC119 vector at the *Pst*I and *Hin*dIII sites. The mutant SCAD expression vectors were subsequently transformed into *E. coli* RS3097 cells (*E. coli* Stock Genetic Center, Yale University) for expression. The remaining SCAD mutant genes (F160Y, F160W, and Y366W) were placed into a T7-7 expression vector under the control of the Φ*10* T7 bacteriophage promoter (*16, 29*). The T7-7 vectors containing the F160Y, F160W, and Y366W mutations were then transformed into an *E. coli* BL21(DE3) (Novagen) host strain as previously described for the wild-type enzyme (*16*). All mutations were confirmed by DNA sequence analysis of the regions containing the mutations (*18*). Additionally, the F160L mutation was confirmed by *Bgl*II digestion as one of the three *Bgl*II sites in the wild-type DNA was removed by the mutation.

Protein Expression and Purification. Transformed BL21-(DE3) and RS3097 *E. coli* cells were grown at 37 °C in Terrific broth (pH 7.0) supplemented with 50 μg/mL ampicillin. The BL21(DE3) cells were allowed to reach an optical density of about 1.0 at 600 nm before the lacUV5 promoter was induced with 0.5 mM isopropyl-β-D-thiogalactoside (IPTG). After 5 h of induction, the BL21(DE3) cells were harvested by centrifugation as previously described (*18*). Induction of the RS3097 cells did not increase yields significantly higher than the basal levels of expression (between 15 and 40 mg of enzyme per 1 L of cell culture). Consequently, these cells were grown to stationary phase (20−24 h) without induction.

The recombinant wild-type SCAD and SCAD mutants were purified from cell paste [RS3097 or BL21(DE3) *E. coli*] according to published procedures (*16, 18*) with minor

modifications to the cell lysis procedure described by DuPlessis et al. (*30*). The final purity of the enzymes was determined to be >95% by sodium dodecyl sulfate (SDS)−polyacrylamide gel electrophoresis. Purified protein was stored in 0.1 mM potassium phosphate (pH 7.0) at −80 °C prior to use.

Materials. The following dyes were used in the electrochemical experiments: methyl viologen (Sigma), indigo disulfonate (Aldrich), pyocyanine [photochemically synthesized (*31*) from phenazine methosulfate (Sigma)], and 8-chlororiboflavin (a generous gift from Dr. J. P. Lambooy, University of Maryland). Butyryl-CoA and crotonyl-CoA were purchased from Sigma. Ferricenium hexafluorophosphate (Aldrich) was prepared according to the method of Lehman and Thorpe (*32*). Glass-distilled water was used to prepare all buffers.

General Methods. Unless indicated otherwise, all experiments were performed in 0.1 M potassium phosphate buffer at pH 7.0. UV−visible spectrophotometric measurements were made on a Perkin-Elmer Lambda 12 spectrophotometer equipped with a thermostated cell compartment to maintain experimental temperatures at 25 °C. Spectra were acquired and manipulated with Perkin-Elmer Computerized Spectroscopy Software (PECSS) version 4.31. All potential values are reported versus standard hydrogen electrode (SHE).

Concentrations of wild-type SCAD and SCAD mutants were measured spectrophotometrically using extinction coefficients determined by the guanidine hydrochloride method of Williamson and Engel (*33*). An extinction coefficient of 14.2 ± 0.4 mM^{-1} cm^{-1} at 451 nm has previously been reported for the uncomplexed, oxidized wild-type SCAD (*16*). For each SCAD mutant, at least five extinction coefficient determinations were made to obtain average values and standard deviations. Extinction coefficients for the crotonyl-CoA-bound oxidized mutants were calculated from spectral changes caused by addition of saturating concentrations (240 μM) of crotonyl-CoA to 14 μM enzyme solutions.

Activity assays were performed at 25 °C using 200 μM ferricenium hexafluorophosphate ($FcPF_6$) as the terminal electron acceptor (*32*). Butyryl-CoA (C_4), hexanoyl-CoA (C_6), or octanoyl-CoA (C_8) served as substrates in the assays. K_m and V_{max} values were determined by varying substrate concentrations from 2 to 200 μM.

Fluorescence Measurements. Excitation (at 450 nm) and emission spectra (480−600 nm) of wild-type SCAD Phe160 mutants were recorded with a Perkin-Elmer LS50B Luminescence Spectrometer. The quantum yields (Q) of enzyme-bound flavins were calculated from the area of the emission spectra as described by Munro and Noble (*34*). Flavin quantum yields of the mutants are presented as a percentage of the wild-type enzyme.

Anaerobic Titration of Wild-Type and Mutant SCAD with Substrate. WT and site-directed mutant enzymes were titrated with butyryl-CoA as described previously (*20*). Approximately 15 μM enzyme in 100 mM potassium phosphate buffer, pH 7.0, was degassed in the cuvette of a spectroelectrochemical cell. The system was then electrochemically reduced—using 100 μM methyl viologen as a mediator—to remove residual oxygen. Aliquots of anaerobic butyryl-CoA (1.6−4.8 mM) were delivered to the enzyme solution through one of the cell ports with a gastight syringe (Hamilton Company, Reno, NV). After a period of 5 min, all spectral changes had occurred, and the spectrum of the enzyme was recorded.

Spectroelectrochemical Methods. The two-electron reduction potential (oxidized/hydroquinone) of each uncomplexed mutant was determined using spectroelectrochemical methods (*35*−*37*). Since the presence of CoA-persulfide is likely to affect the redox properties of the flavin cofactor, only inhibitor-free enzyme was used in the electrochemical experiments. Methyl viologen (100 μM) was added to each enzyme solution (10−20 μM) to mediate electron transfer from the gold working electrode to the enzyme-bound flavin. Additionally, the following indicator dyes (2−5 μM) were used to facilitate equilibration between the protein and working electrode: pyocyanine (E_m = −18 mV, pH 7.0), indigo disulfonate (E_m = −102 mV, pH 7.0), and 8-chlororiboflavin (E_m = −142 mV, pH 7.0). Contents of the spectroelectrochemical cell were deoxygenated by repeated cycles of evacuation and refilling with ultrapure argon. Approximately 1.5 mC of charge was introduced at each point in the reductive titration from a Bioanalytical Systems (BAS) 50CV electrochemical analyzer. Equilibration between the dyes and enzyme typically took 1−2 h and was defined by a change in potential of <1 mV/10 min.

Experiments to determine the midpoint potential of the mutant SCAD in the presence of butyryl-CoA (BCoA) and crotonyl-CoA (CCoA) were performed as described by Stankovich and Soltysik (*20*). The cuvette of the spectroelectrochemical cell contained approximately 15 μM enzyme, 100 μM methyl viologen, 2 μM indigo disulfonate, and 5 μM pyocyanine in standard buffer. A 100 μL solution of BCoA and CCoA (12 mM each) was placed in the sidearm of the cell. After the cell contents were degassed, the enzyme and dyes were electrochemically reduced to a point near the expected equilibrium potential. Next, the solution in the sidearm was tipped into the cuvette, diluting the BCoA and CCoA concentrations to 150 μM each. The system came to equilibrium after ∼1 h, and the visible spectrum of the solution was recorded.

Calculations. The concentrations of enzymes in various oxidation and ligation states were calculated from the spectral data using multicomponent linear regression analysis. In many cases, it was necessary to remove the spectral contributions from indicator dyes and/or turbidity before proceeding with the calculations (*14*). After these corrections, the midpoint potentials for the enzymes were determined from the Nernst equation:

$$E = E_m + 2.303\frac{RT}{nF}\log\frac{[\text{oxidized}]}{[\text{reduced}]} \qquad (1)$$

where E is the measured potential at each point in the titration, E_m is the midpoint potential, R is the gas constant (8.31441 J mol^{-1} K^{-1}), T is the temperature in degrees kelvin, n is the number of electrons transferred in the reaction, and F is Faraday's constant (96 485 C mol^{-1}). Typical error for experimentally determined midpoint potentials is ±2−5 mV (*14*).

The midpoint potentials for uncomplexed mutant enzymes were extracted from linear regression analysis of Nernst plots (E vs log [oxidized]/[reduced]) constructed from potentiometric titration data. Midpoint potentials for enzymes in the

presence of the butyryl/-crotonyl-CoA couple were determined from one point per experiment. Because BCoA and CCoA were in large excess over enzyme concentrations, the system potential (E) equilibrated near the midpoint potential of the free BCoA/CCoA couple (−13 mV) (*20*). Using E and the concentrations of oxidized and reduced enzyme complexes, E_m was calculated from eq 1, assuming that the number of electrons required for complete flavin reduction (n) was 2 (*20*).

RESULTS AND DISCUSSION

Expression and Characterization of Purified Wild-Type and Mutant SCAD. All mutant enzymes were overexpressed in sufficiently high yield (20−50 mg of protein per 1 L of culture) in either BL21(DE3) or RS3097 *E. coli* cells. The enzymes were purified to homogeneity and showed distinct 44 kDa SDS−polyacrylamide gel bands similar to the wild-type enzyme. With the exception of Y366W, all SCAD mutants were purified as oxidized holoproteins as evidenced by their bright yellow or green color. The Y366W mutant exhibited no color, indicating the absence of a tightly bound FAD cofactor. Attempts to reconstitute this mutant with FAD at various stages during purification were unsuccessful. This result was not surprising, however, given the location and orientation of Tyr366 relative to the flavin (see Figure 1). Others have shown that incorporation of bulky residues in the active sites of ACDs often compromises the flavin binding capacity of the enzyme (*38*).

Two of the mutants, Y366F and F160W, were purified in a green form, indicating the presence of an enzyme-bound CoA-persulfide. Usually this inhibitor can easily be released from the active site of the enzyme with the aid of a thiopropyl-Sepharose column (*39*). However, when the Y366F mutant was passed through this column, the 2-thiopyridone leaving group became tightly bound to the protein and could not be removed without denaturing the enzyme. This irreversible binding was not found in any other SCAD mutants. It is possible that in Y366F, the ringed thiopyridone molecule is engaged in π-stacking interactions with aromatic groups and/or the flavin ring, increasing the affinity for the complex. Indeed, preliminary modeling studies of the Y366F mutant suggest that once the hydrogen bond to Gln253 is removed, the phenyl group may rotate into a more coplanar orientation with the flavin cofactor to provide a more hydrophobic active site. Since CoA-persulfide/thiopyridone-free Y366F SCAD could not be obtained, this mutant was not used for subsequent spectroelectrochemical studies.

The spectral properties of the CoA-persulfide-free enzymes (oxidized) are nearly identical to those of the wild-type enzyme, suggesting that overall, the flavin binding region of the enzyme is unaltered by the mutations. Extinction coefficients and absorbance maxima of each mutant are presented in Table 1. The lack of significant changes in the visible spectra of the mutants is anticipated since only the environment around the *o*-xylene ring is affected by mutations at the 160 position. Solvent molecules are not able to form hydrogen bonds with the atoms in the *o*-xylene subnucleus of the flavin (*41*), so displacement of water molecules by increasing the size of the aromatic ring is unlikely to significantly change the flavin spectrum. In cases where hydrogen bonding interactions between the flavin and surrounding environment (protein or solvent) are removed, the absorbance maxima of the transition 2 band become slightly red-shifted and more intense. Likewise, removal of the aromatic residue by substitution with a leucine does not appear to cause *increased* hydrogen bonding interactions between the flavin and solvent. As the environment surrounding the isoalloxazine ring becomes increasingly solvated, the 450 nm band is generally shifted to lower wavenumbers (*40*).

Table 1: Spectral Properties[a] of Oxidized Wild-Type and Mutant *M. elsdenii* SCAD

	λ_{max} (nm)		ϵ_λ (mM^{-1} cm^{-1})		
enzyme	1	2	1	2	$\epsilon_{280}/\epsilon_{450}$
WT	378	451	9.5 ± 0.3	14.2 ± 0.4[b]	4.0
F160Y	380	453	9.8 ± 0.3	14.4 ± 0.4	4.6
F160W	380	451	10.0 ± 0.4	13.9 ± 0.5	4.5
F160L	377	452	10.3 ± 0.2	13.9 ± 0.2	5.5
Y366L	380	450	10.3 ± 0.2	14.4 ± 0.2	3.9
Y366F[c]	349	443	12.2 ± 0.1	13.6 ± 0.1	12.2

[a] Maximum wavelength (λ_{max}) and extinction coefficient (ϵ_λ) at each major electronic transition (1 and 2). [b] From reference (*16*). [c] Determined for CoA-persulfide-bound Y366F.

Fluorescence. Spectral changes due to mutations around the *o*-xylene ring are more evident from the fluorescence emission studies. Substitution of a tryptophan at the 160 position causes the quantum yield (Q) for flavin fluorescence to *decrease* by 30% relative to the wild-type enzyme (0.007 vs 0.010), consistent with stronger stacking interactions between the tryptophan and the oxidized isoalloxazine ring. On the other hand, when the aromatic residue is removed by mutation to a leucine, *Q increases* by 20% to 0.012. Even still, fluorescence in the F160L mutant is strongly quenched relative to uncomplexed FAD ($Q = 0.03$) (*34*) as a result of strong apoprotein−flavin interactions with other residues in the active site.

Activities and Substrate Specificities. The catalytic properties of wild-type and SCAD mutants toward substrates of varying chain length were measured using the method of Lehman and Thorpe (*32*) and are summarized in Table 2. Ferricenium hexafluorophosphate was chosen for the assays since the positively charged (oxidized) molecule is believed to interact with ACDs similar to electron-transferring flavoprotein (ETF), the physiological electron acceptor (*32*). All of the enzymes exhibit the highest activity toward four-carbon substrates, with the V_{max} of the mutants somewhat lower than the wild-type enzyme. The Phe160 mutants have similar kinetic parameters when compared with each other, although their V_{max} values are only about one-third of the wild-type enzyme for C_4-CoA substrates.

Mutations to tyrosine-366 have more interesting effects on the specific activity of the enzyme. This is not unexpected considering that Tyr366 is located in the bottom of the substrate binding cavity (*19*). It should be noted that the activity of Y366F was measured with the green form of the enzyme. Since the enzyme is only partially bound (44%) with CoA-persulfide, and the total concentration of the partially bound enzyme in the assay is much lower than the substrate concentration (30 nM versus 2−200 μM), the presence of the inhibitor will not significantly affect the kinetic parameters. While mutating the tyrosine to a phenylalanine causes only minor changes in V_{max} and K_m, replacing the tyrosine with a leucine results in a K_m that is nearly

Table 2: Kinetic Parameters[a] of Wild-Type and Mutant *M. esldenii* SCAD with Butyryl-CoA (C_4), Hexanoyl-CoA (C_6), and Octanoyl-CoA (C_8)

enzyme	parameter	butyryl-CoA, C_4	hexanoyl-CoA, C_6	octanoyl-CoA, C_8
wild-type	K_m (μM)	65 ± 8	76 ± 5	170 ± 65
	V_{max} (s^{-1})[b]	33 ± 2	3.2 ± 0.1	0.8 ± 0.2
	V_{max}/K_m ($mM\ s^{-1}$)	507 ± 70	42 ± 3	5 ± 2
F160L	K_m (μM)	69 ± 7	35 ± 3	93 ± 28
	V_{max} (s^{-1})	11.8 ± 0.6	0.28 ± 0.01	0.37 ± 0.07
	V_{max}/K_m ($mM\ s^{-1}$)	171 ± 19	8.0 ± 0.7	4 ± 1
F160Y	K_m (μM)	107 ± 25	17 ± 3	198 ± 93
	V_{max} (s^{-1})	12.5 ± 1.6	0.13 ± 0.01	0.40 ± 0.01
	V_{max}/K_m ($mM\ s^{-1}$)	117 ± 33	8 ± 2	2 ± 1
F160W	K_m (μM)	106 ± 11	20 ± 2	86 ± 56
	V_{max} (s^{-1})	12.4 ± 0.7	0.22 ± 0.01	0.24 ± 0.09
	V_{max}/K_m ($mM\ s^{-1}$)	117 ± 14	11 ± 1	3 ± 2
Y366L	K_m (μM)	117 ± 12	43 ± 12	87 ± 8
	V_{max} (s^{-1})	3.9 ± 0.2	0.11 ± 0.01	0.11 ± 0.01
	V_{max}/K_m ($mM\ s^{-1}$)	33 ± 4	2.5 ± 0.7	1.3 ± 0.2
Y366F[c]	K_m (μM)	55 ± 11	82 ± 9	118 ± 46
	V_{max} (s^{-1})	25.4 ± 2.8	5.8 ± 0.3	1.2 ± 0.3
	V_{max}/K_m ($mM\ s^{-1}$)	462 ± 108	70 ± 9	10 ± 5

[a] Determined at 25 °C in 100 mM potassium phosphate (pH 7) using 200 μM ferricenium. [b] V_{max} expressed in $[FcPF_6]\cdot[FAD]^{-1}\ s^{-1}$. [c] Determined for CoA-persulfide-bound Y366F SCAD.

double and a V_{max} is lowered to only 12% of wild-type SCAD. Of all the mutants created for this work, Y366L is clearly the most catalytically inefficient with a V_{max}/K_m value of only 33 ± 4 $mM^{-1}\ s^{-1}$. More interesting is the activity that Y366F SCAD has toward 6- and 8-carbon substrates. While the V_{max}/K_m values with C_4 substrates are similar for Y366F and wild-type SCAD, with the longer substrates the V_{max}/K_m value of the mutant is twice that of the wild-type enzyme. Removal of the phenolic hydroxyl group may allow the enzyme to accommodate substrate of longer chain lengths (see Figure 1).

Midpoint Potentials of Uncomplexed Wild-Type and Mutant SCAD. The two-electron reduction potentials for mutant bound flavins ($E_{ox/hq}$) were measured at pH 7.0 using standard spectroelectrochemical techniques (*16*, *35*). As a control, the potential of the wild-type SCAD was redetermined under the same experimental conditions. The spectral changes that occurred during this titration were identical to those observed previously (*16*, *35*), with <5% of the flavin thermodynamically stabilized in the semiquinone form. An average midpoint potential of −79 ± 4 mV was obtained for the wild-type enzyme (Table 3), a value that is within experimental error of the previously reported values for native (−79 mV) (*15*) and recombinant *M. elsdenii* SCAD (−76 and −75 mV) (*16*, *18*).

A representative potentiometric titration of the F160Y SCAD mutant is shown in Figure 2. From a linearized Nernst plot of the spectral and electrochemical data (inset, Figure 2), a midpoint potential of −109 mV was obtained for the $E_{ox/hq}$ couple. Like all of the mutants in the current study, the spectral changes that occur to F160Y are remarkably similar to those occurring in the wild-type enzyme. Less than 5% semiquinone accumulates during the titration of each mutant, with the exception of F160L SCAD (6.5%). The low

Table 3: Midpoint Potentials[a] for Wild-Type and Mutant *M. elsdenii* SCAD

enzyme	$E_{ox/hq}$ (free)	% Sq[b]	$\hat{E}_{ox/hq}$ (bound)[c]	$\Delta E_{ox/hq}$
FAD[d]	−219	<5.0	–	–
WT	−75,[e] −79 ± 4[f]	<5.0	−19 ± 3	+60 ± 5
F160Y	−111 ± 5	<5.0	−57 ± 3	+54 ± 6
F160W	−122 ± 4	<5.0	−54 ± 3	+68 ± 5
F160L	−133 ± 5	6.5	−34 ± 3	+99 ± 6
Y366L	−123 ± 4	<5.0	−47 ± 3	+76 ± 5

[a] Potentials reported in mV at 25 °C in 100 mM potassium phosphate buffer, pH 7.0. [b] Maximum percentage of enzyme stabilized in blue neutral semiquinone form during potentiometric titration of uncomplexed enzyme. [c] Potential determined in the presence of butyryl-CoA (150 μM) and crotonyl-CoA (150 μM). [d] From reference (*17*). [e] From reference (*16*). [f] Average of six determinations (from this work).

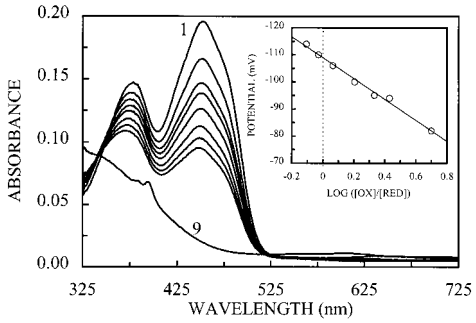

FIGURE 2: Potentiometric titration of uncomplexed F160Y SCAD (13.6 μM). Titration was performed under anaerobic conditions at 25 °C in 100 mM potassium phosphate buffer, pH 7.0, containing 100 μM methyl viologen. Indigo disulfonate (2 μM) and pyocyanine (5 μM) were used as indicator dyes. Curve 1, fully oxidized spectrum. Curves 2−8: E = −82, −94, −95, −100, −106, −110, and −114 mV. Curve 9, fully reduced spectrum. Spectral contributions from the indicator dyes have been subtracted. Inset: Nernst plot indicating E_m = −109 mV.

amounts of thermodynamically stabilized semiquinone indicate that the potentials for the individual electron-transfer reactions are separated by at least 120 mV, with the first ($E_{ox/sq}$) transfer being more negative than the second ($E_{sq/hq}$). While the spectral changes are similar to wild-type SCAD, the two-electron reduction potentials of all the mutants are 32−54 mV more negative (Table 3). This result was somewhat surprising since aromatic residues were removed in some mutants (F160L and Y366L) and retained in others (F160Y and F160W). It was expected that if the π-stacking interactions were important for shifting the potential of the flavin positive from −219 mV (the value for free FAD in solution at pH 7.0), then increasing these interactions with larger aromatic groups should cause the potential to become even more positive.

Why Are the Potentials for F160Y and F160W More Negative than Wild-Type SCAD? This question can best be addressed by considering the geometrical requirements for strong interactions between aromatic groups and the position of the phenyl ring relative to the *o*-xylene ring of the flavin (Figure 1). These requirements have been described in detail by Hunter and Sanders (*42*) using an atomic charge model. One of their key findings was that favorable aromatic stacking interactions occur only when attractive $\pi-\sigma$ interactions are able to overcome repulsive $\pi-\pi$ interactions (*42*). In a face-to-face orientation, the partially negative charged faces of the π-electron clouds come in contact with each other and, as a result, electrostatic repulsion dominates. On the other hand, when the two aromatic rings are offset or

perpendicular to one another, the positively charged σ-framework of one ring attracts the negatively charged π-system of the other, and favorable interactions dominate. In the flavin binding region of SCAD (Figure 1), it is clear that the geometry of the isoalloxazine ring and Phe160 cannot be explicitly classified as face-to-face or perpendicular. The phenyl ring is slightly offset from the *o*-xylene ring, and inclined at an angle of 25−35° relative to the flavin. Consequently, the phenylalanine is likely to engage in both attractive and repulsive interactions with the flavin.

According to this interpretation, replacement of the phenylalanine with a tryptophan or a tyrosine should lead to increased contributions from repulsive $\pi-\pi$ interactions. Unlike phenylalanine, the ring systems of tyrosine and tryptophan contain electron-donating heteroatoms. When the flavin is oxidized, interactions between the xylene ring and the aromatic residues are likely to be energetically neutral, or even somewhat favorable, as a result of $\pi-\sigma$ interactions (*13*). However, when the enzyme-bound flavin is reduced by two electrons, a formal negative charge develops on the pyrimidine ring and strong $\pi-\pi$ repulsion between the flavin and the electron-rich aromatic residues begins to dominate. Weaker binding of the anionic hydroquinone will result in a lowered $E_{ox/hq}$ value. The potential of the F160W mutant is 11 mV even more negative than F160Y, consistent with the fact that the tryptophan indole ring is more electron-rich than the phenolic ring of tyrosine.

Removal of both attractive and repulsive interactions by mutating the phenylalanine to a leucine also causes $E_{ox/hq}$ to shift negative (−54 mV) relative to wild-type enzyme (Table 3). This result suggests that, overall interactions between phenylalanine and the flavin are quite favorable for formation of the anionic hydroquinone. A similar argument is made for the tyrosine at position 366. The T-shaped orientation of the phenolic ring of this residue with the *o*-xylene subnucleus of the flavin provides very strong $\pi-\sigma$ interactions with the reduced flavin. In this orientation, contributions from repulsive $\pi-\pi$ interactions should be negligible. Indeed, removal of the favorable interactions by replacing the tyrosine with a leucine causes $E_{ox/hq}$ to become considerably more negative (by −44 mV).

Midpoint Potentials of Butyryl-CoA/Crotonyl-CoA Complexed SCAD Mutants. Previous redox studies have shown that substrate/product binding causes the midpoint potential of wild-type *M. elsdenii* SCAD to increase by 60 mV (*20*). As a result, the flavin ($E_{ox/hq} = -19$ mV) becomes nearly isopotential with the substrate/product couple ($E_{BCoA/CCoA} = -13$ mV) (*20*), suggesting that the binding of substrate and/or product is important for the regulation of electron transfer. Subsequent spectroelectrochemical and Raman studies of MCAD·analogue complexes indicate that hydrogen bond induced polarization of product is at least partially responsible for the positive shift (*23*, *43*). Similar redox potential modulation is likely to occur in the SCAD mutants under current investigation. However, larger shifts may be required for catalytic activity since all of the mutants have uncomplexed potentials significantly more negative than the wild-type enzyme (see Table 3).

To determine if the redox potentials of the mutant-bound flavins are modulated to larger degrees, a conditional midpoint potential ($\hat{E}_{ox/hq}$) was determined for each mutant in the presence of BCoA (150 μM) and CCoA (150 μM).

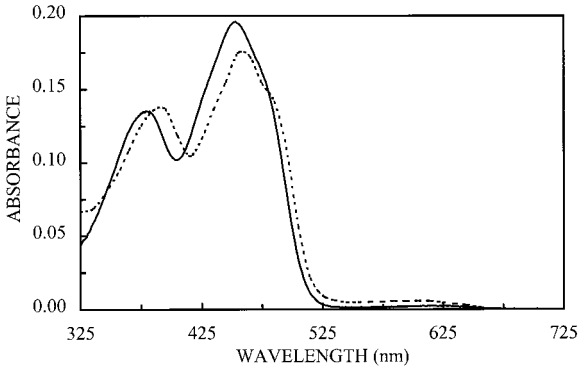

FIGURE 3: Spectra of F160Y SCAD (13.6 μM) before (—) and after (- - -) the addition of butyryl-CoA and crotonyl-CoA (final concentrations = 150 μM each). The potential of the system after addition of the 1:1 BCoA/CCoA mixture was −24 mV versus SHE. The experiment was performed under anaerobic conditions at 25 °C in 100 mM potassium phosphate buffer, pH 7.0, containing 100 μM methyl viologen, 2 μM indigo disulfonate, and 5 μM pyocyanine. Spectral contributions from indigo disulfonate and pyocyanine have been subtracted.

The experiments were performed (see Materials and Methods) using a method that was identical to that used for the wild-type enzyme (*20*). Addition of the 1:1 BCoA/CCoA mixture from the sidearm of the cell resulted in varying degrees of flavin bleaching and small changes in the cell potential. The spectral and potential changes were stabilized after a short period of time (<1 h). Figure 3 shows the spectral changes that occurred during an experiment with F160Y SCAD. After subtracting the spectral contributions from pyocyanine and indigo disulfonate, it is clear that there is long-wavelength absorbance that is characteristic of a charge-transfer band between the reduced flavin and CCoA. The change in absorbance at 453 nm is 37% of the change that occurs upon addition of a 1:1 mixture of BCoA/CCoA to wild-type SCAD (*20*).

The concentrations of the relevant enzyme species at equilibrium were calculated from the absorbance of the transition 2 bands (453 nm for F160Y) and the absorbance at 580 nm. For the uncomplexed mutants (oxidized), the extinction coefficients of the transition 2 bands are provided in Table 1. Extinction coefficients for the CCoA-bound mutants were found to be slightly lower: F160Y ($\epsilon_{453} = 13.2$ mM^{-1} cm^{-1}), F160W ($\epsilon_{451} = 13.1$ mM^{-1} cm^{-1}), F160L ($\epsilon_{452} = 12.8$ mM^{-1} cm^{-1}), and Y366L ($\epsilon_{450} = 13.3$ mM^{-1} cm^{-1}).

Both BCoA and CCoA are thought to bind tightly to the reduced form of wild-type SCAD (*16*, *20*). We assumed similar tight binding to the SCAD mutants, and thus no free reduced enzyme should exist at equilibrium. The extinction coefficients for the BCoA-bound reduced mutants ($\epsilon_{450} = 2.0$ mM^{-1} cm^{-1}) and the CCoA reduced mutants ($\epsilon_{450} = 4.0$ mM^{-1} cm^{-1} and $\epsilon_{580} = 3.0$ mM^{-1} cm^{-1}) were assumed to be the same as those obtained from stopped-flow studies with mammalian MCAD (*44*).

For the F160Y SCAD mutant bound to BCoA/CCoA (Figure 3), the total concentrations of oxidized and reduced enzyme were determined to be 12.7 and 1.0 μM, respectively. From the Nernst equation (eq 1) and the system potential ($E = -24$ mV), an $\hat{E}_{ox/hq}$ of −57 mV can be calculated. Thus, binding of the BCoA/CCoA mixture causes a +54 mV potential shift from the uncomplexed $E_{ox/hq}$ value of −111 mV, a shift that is remarkably similar to that determined for

wild-type SCAD (+60 mV) (*20*). BCoA/CCoA complexed $\hat{E}_{ox/hq}$ values were determined for the other SCAD mutants in a similar manner and are summarized in Table 3. Unlike the F160Y mutant, these shifts are all significantly larger than the wild-type enzyme, with the greatest shift occurring in the F160L mutant (+99 ± 6 mV).

At this point it is premature to speculate on the cause(s) of the variations in potential shifts. However, it is interesting that those mutants with the most negative uncomplexed potentials (F160L and Y366L) undergo the most positive potential shifts when complexed with BCoA/CCoA. It is quite possible that these shifts are needed to drive the flavin potential close enough to the potential of the BCoA/CCoA couple (−13 mV) such that some activity is maintained (Table 2).

Effect of Binding on the Potential of the Butyryl-CoA/Crotonyl-CoA Couple. Although BCoA/CCoA binding raises the midpoint potentials of all of the mutants considerably, the $E_{ox/hq}$ values are still significantly lower than the potential of the free BCoA/CCoA couple ($E_{BCoA/CCoA} = -13$ mV). For the F160Y mutant, the potential difference is 44 mV, which represents a 2.0 kcal mol^{-1} energy barrier for the two-electron-transfer reaction. This energy barrier can be lowered even further if product is stabilized by binding, i.e., a *negative* $E_{BCoA/CCoA}$ shift. Unfortunately, it is very difficult to directly measure the redox potentials of enzyme-bound acyl-CoA and 2-enoyl-CoA thioesters using conventional spectroelectrochemical techniques. The visible spectral profiles of these substrate/product couples differ from each other only slightly ($\epsilon_{260} = 16.4$ mM cm^{-1} for BCoA versus $\epsilon_{260} = 22.6$ mM cm^{-1} for CCoA) (*45*) and in a region where there are large spectral contributions from the enzyme ($\epsilon_{260} = 54$ mM cm^{-1} for wild-type SCAD). However, the potential differences ($\Delta\hat{E}$) between $E_{BCoA/CCoA}$ and $\hat{E}_{ox/hq}$ in the complexes can be easily estimated if the equilibrium constants for the electron-transfer reactions are known. The midpoint potentials for the butyryl-CoA/crotonyl-CoA couples bound to the enzyme can then be back-calculated using $\hat{E}_{ox/hq}$ values in Table 3. Stankovich and Soltysik have shown that anaerobic titrations of ACDs with substrate provide a convenient way to obtain $\Delta\hat{E}$ values (*20*).

Figure 4A shows the progress of a titration of wild-type SCAD with BCoA. Addition of the substrate results in bleaching of the flavin chromophore with a corresponding increase in absorbance between 515 and 700 nm. The appearance of a long-wavelength band, centered at 580 nm, is attributed to the formation of a charge-transfer complex between the highest occupied molecular orbital (HOMO) of the flavin and the lowest unoccupied molecular orbital (LUMO) of the polarized crotonyl-CoA product (*1*, *22*, *46*). Reduction of the 451 nm band is not linear with respect to the amount of BCoA added, and a clear break point at 1 equiv of BCoA is noticeably absent (see inset of Figure 4A). These results are consistent with the reductive half-reaction model proposed by Thorpe et al. (*47*) (Scheme 1) in which six enzyme species are in equilibrium: $EFAD_{ox}$, $EFAD_{red}$, $EFAD_{ox}$·BCoA, $EFAD_{ox}$·CCoA, $EFAD_{red}$·BCoA, and $EFAD_{red}$·CCoA.

At the 1 equiv point, however, most of the enzyme will be complexed with either BCoA or CCoA such that the predominant enzyme species are $EFAD_{ox}$·BCoA and $EFAD_{red}$·CCoA. This argument was made by Thorpe et al. (*47*) and

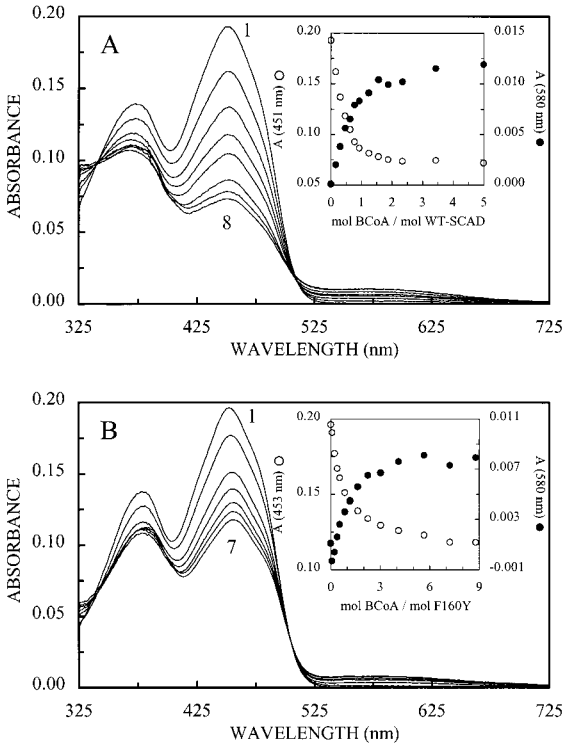

FIGURE 4: Reductive titration of wild-type SCAD and F160Y SCAD with butyryl-CoA. Titrations were performed under anaerobic conditions at 25 °C in 100 mM potassium phosphate buffer, pH 7.0, containing 100 μM methyl viologen. (A) Titration of wild-type SCAD (13.6 μM) with butyryl-CoA. Only selected spectra are shown for clarity. Curves 1−8: [butyryl-CoA] = 0.0, 2.3, 4.2, 6.3, 8.4, 12.6, 20.9, and 31.2 μM, respectively. Inset: Plot of absorbance at 451 nm (○) and 580 nm (●) as a function of the moles of butyryl-CoA added per mole of enzyme. (B) Titration of F160Y SCAD (13.6 μM) with butyryl-CoA. Only selected spectra are shown for clarity. Curves 1−7: [butyryl-CoA] = 0.0, 3.2, 11.6, 22.0, 40.3, 73.8, and 122.4 μM, respectively. Inset: Plot of absorbance at 453 nm (○) and 580 nm (●) as a function of the moles of butyryl-CoA added per mole of enzyme.

holds true for FAD reduction and oxidation by tight binding substrates and products. Both BCoA and CCoA are presumed to bind rather tightly to oxidized and reduced SCAD on the basis of K_ds measured with the kinetically dead enzyme E367Q ($E367Q_{ox}$·BCoA, $K_d = 6.2$ μM; and $E367Q_{red}$·CCoA, $K_d = 0.19$ μM) (*16*). Consequently, the amount of flavin reduction that occurs at 1 equiv of BCoA is a reflection of the internal equilibrium (K_2) between $EFAD_{ox}$·BCoA and $EFAD_{red}$·CCoA (*47*). From K_2, a conditional midpoint potential difference ($\Delta\hat{E}$) between the substrate/product couple and the enzyme-bound flavin can be calculated:

$$\Delta\hat{E} = -2.303\frac{RT}{nF}\log(K_2) \qquad (2)$$

Addition of 1 equiv of butyryl-CoA to a buffered solution containing wild-type SCAD results in 66% flavin bleaching (curve 6, Figure 4A), or a K_2 value of 1.9. This corresponds to an $\Delta\hat{E}$ value of −8 mV, with the potential of the enzyme-bound substrate/product couple more negative than the flavin. Therefore, electron transfer from substrate to flavin is now slightly *favored*—by 0.4 kcal mol^{-1}. For the F160Y mutant, the addition of 1 equiv of BCoA (curve 3, Figure 4B) causes only 29% flavin reduction ($K_2 = 0.41$). This indicates that the midpoint potential of the BCoA/CCoA couple in the

Scheme 1: Equilibrium Model for ACDs in the Presence of Butyryl-CoA and Crotonyl-CoA [Adapted from Reference (*47*)]

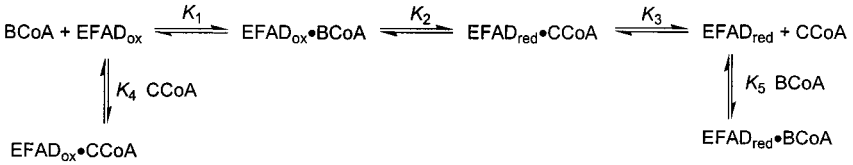

Table 4: Percent Reduction[a] for Wild-Type and Mutant *M. elsdenii* SCAD Using Butyryl-CoA

enzyme	% bleaching 1:1 BCoA/enzyme	% bleaching excess BCoA	K_2[b]	$\Delta\hat{E}$ (mV)[c]
WT	66	74	1.9	-8 ± 3
F160Y	29	47	0.41	$+11 \pm 3$
F160W	34	44	0.52	$+8 \pm 3$
F160L	25	36	0.33	$+14 \pm 3$
Y366L	3.4	15	0.035	$+43 \pm 3$

[a] Based on reduction of the transition 2 flavin band at 25 °C in 100 mM potassium phosphate, pH 7.0. [b] Internal equilibrium constant (see Scheme 1). [c] Conditional potential difference between the BCoA/CCoA couple and the flavin oxidized/hydroquinone couple.

active site of F160Y is still more positive (+11 mV) than the flavin potential. It should be noted that for all enzymes in this study, the flavin continues to be reduced after the 1 equiv point. Past the 1 equiv point, free BCoA begins to compete with CCoA for the reduced enzyme, and the equilibrium for the reaction (K_2) becomes disrupted (*47*).

The percent reduction and $\Delta\hat{E}$ values for the other SCAD mutants are summarized in Table 4. Most notable is the lack of significant flavin bleaching of the Y366L SCAD mutant—only 3.4% at 1 equiv of BCoA/mol of enzyme. The large potential separation between the flavin and substrate/product couple ($+43 \pm 3$ mV) is consistent with the Y366L mutant having the lowest V_{max}/K_m value (33 ± 4 mM s^{-1} with BCoA) and may be attributed to changes in the substrate binding cavity of the enzyme. Substitution of a leucine at the 160 position should cause the active site to become more open and solvated, and as a result, BCoA may not be oriented in the active site of the mutant in a position that favors electron transfer from substrate to the flavin.

From the $\hat{E}_{ox/hq}$ (bound) and $\Delta\hat{E}$ values in Table 4, the potential of the enzyme-bound BCoA/CCoA couple can be obtained. For wild-type SCAD, the potential of the couple is −27 mV, which means that $E_{BCoA/CCoA}$ is lowered by 14 mV in the active site of the enzyme. This 14 mV shift is represented by the solid bar in Figure 5. It is not surprising that the potential of the substrate/product couple is also affected by binding. A considerable number of recent studies (*21*−*23*, *48*−*51*) have shown that the ground-state electronic properties of CoA−product analogues are strongly influenced by interactions with ACDs. Upon binding, two hydrogen bonds are formed between the thioester carbonyl oxygen and the ACD, one from the 2′-OH group of the flavin and the other from the amide backbone of an active site glutamate (E367) (*19*). The analogue is then polarized such that partial positive charge develops near the N(5) atom of the flavin. This leads to formation of a charge-transfer complex between the electron-rich reduced flavin and electron-deficient C(2)═C(3) region of the ligand. As one could imagine, formation of this CT complex with natural 2-enoyl-CoA products should stabilize the C(2)═C(3) double bond; i.e., reduction of the bond should be *thermodynamically* more difficult.

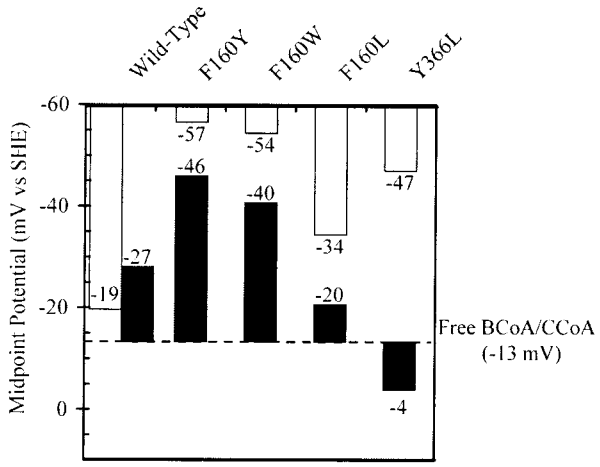

FIGURE 5: Comparison of the butyryl-CoA/crotonyl-CoA and flavin midpoint potentials in the SCAD·BCoA/CCoA complexes. The solid bars show the midpoint potential shifts for the BCoA/CCoA couple upon binding. The unfilled bars indicate the midpoint potential shifts for the flavin oxidized/hydroquinone potential ($E_{ox/hq}$) in the complex.

Thus, $E_{BCoA/CCoA}$ is expected to be lowered by binding to the ACDs.

The potential shifts for the BCoA/CCoA couple bound to F160Y and F160W SCAD are even greater than the shift in wild-type SCAD (solid bars, Figure 5), indicating that these mutants are better able to activate acyl-CoA substrates and 2-enoyl-CoA products. A possible explanation for this behavior is that electrostatic interactions between the aromatic residue, the isoalloxazine ring of the flavin, and CCoA affect the extent to which product is stabilized. The flavin cofactor in F160Y and F160W SCAD is expected to be more electron-rich than in the wild-type enzyme due to interaction with the tyrosine and tryptophan electron-donating heteroatoms. As a result, stronger charge-transfer interactions between the reduced flavin and the polarized crotonyl-CoA may develop (Figure 6). This would cause crotonyl-CoA to become even more thermodynamically stabilized and result in a larger negative $E_{BCoA/CCoA}$ shift.

Product formation actually appears to be made more *difficult* by binding to the Y366L mutant, as evidenced by the 9 mV *positive* $E_{BCoA/CCoA}$ shift. This result is consistent with the idea that the substrate binding cavity does not allow for favorable formation of the CT complex. However, until crystallographic studies with the Y366L mutant have been completed, the specific arrangement of the ligand and flavin in the mutant will remain unclear.

CONCLUSION

The results of our redox studies with the SCAD mutants demonstrate the importance of aromatic stacking interactions for both flavin and substrate/product activation. The ring systems of the two residues under investigation were found to have the ideal chemical properties for stabilizing the

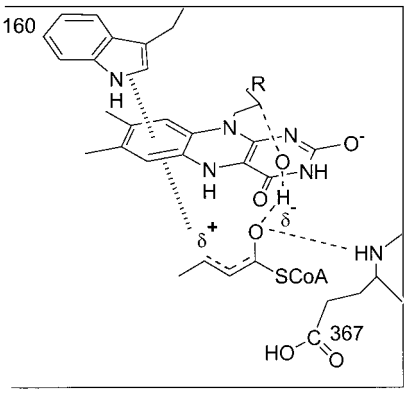

FIGURE 6: Model of F160W SCAD shown with polarized crotonyl-CoA bound in the active site. Tryptophan and crotonyl-CoA are on the *si*- and *re*-sides of the flavin, respectively. An electronegative aromatic residue at position 160 (tryptophan or tyrosine) may help stabilize the formation of partial positive charge on C(3) of crotonyl-CoA.

reduced flavin. Mutation of either Phe160 or Tyr366 to a nonaromatic residue caused $E_{ox/hq}$ to shift negative, toward that of the free FAD (−219 mV). Replacement of Phe160 with electron-rich aromatic residues also destabilized the reduced flavin, suggesting that one reason for the lower potential of mammalian MCAD is the incorporation of a tryptophan at the 166 position—equivalent to position 160 in *M. elsdenii* SCAD. However, it is important to recognize that other noncovalent apoprotein−flavin interactions undoubtedly influence the midpoint potential of the flavin. The side chains and peptide backbones of several residues surrounding the pyrimidine subnucleus of the flavin could potentially serve as hydrogen bond donors or acceptors (*19*).

REFERENCES

1. Engel, P. C., and Massey, V. (1971) *Biochem. J. 125*, 889−902.
2. Shaw, L., and Engel, P. C. (1984) *Biochem. J. 218*, 511−520.
3. Finocchiaro, G., Ito, M., and Tanaka, K. (1987) *J. Biol. Chem. 262*, 7982−7989.
4. Engel, P. C., Williamson, G., and Shaw, L. (1984) in *Flavins and Flavoproteins 1983* (Bray, R. C., Engel, P. C., and Mayhew, S. G., Eds.) pp 403−412, Walter de Gruyter, Berlin.
5. Elsden, S. R., Gilchrist, F. M. C., Lewis, D., and Volcani, B. E. (1951) *Biochem. J. 49*, 1xix−1xx.
6. Elsden, S. R., and Lewis, D. (1953) *Biochem. J. 55*, 183−189.
7. Swenson, R. P., and Krey, G. D. (1994) *Biochemistry 33*, 8505−8514.
8. Breinlinger, E. C., and Rotello, V. M. (1997) *J. Am. Chem. Soc. 119*, 1165−1166.
9. Palfey, B. A., Moran, G. R., Entsch, B., Ballou, D. P., and Massey, V. (1999) *Biochemistry 38*, 1153−1158.
10. Cuello, A. O., McIntosh, C. M., and Rotello, V. M. (2000) *J. Am. Chem. Soc. 122*, 3517−3521.
11. Bradley, L. H., and Swenson, R. P. (1999) *Biochemistry 38*, 12377−12386.
12. Chang, F.-C., and Swenson, R. P. (1999) *Biochemistry 38*, 7168−7176.
13. Zhou, Z., and Swenson, R. P. (1996) *Biochemistry 35*, 15980−15988.
14. Johnson, B. D. (1993) Ph.D. Thesis, University of Minnesota, Minneapolis, MN.
15. Fink, C. W., Stankovich, M. T., and Soltysik, S. (1986) *Biochemistry 25*, 6637−6643.
16. Becker, D. F., Fuchs, J. A., and Stankovich, M. T. (1994) *Biochemistry 33*, 7082−7087.
17. Lowe, H. J., and Clark, W. M. (1956) *J. Biol. Chem. 221*, 983.
18. Becker, D. F., Fuchs, J. A., Banfield, D. K., Funk, W. D., MacGillivray, R. T. A., and Stankovich, M. T. (1993) *Biochemistry 32*, 10736−10742.
19. Djordjevic, S., Pace, C. P., Stankovich, M. T., and Kim, J.-J. (1995) *Biochemistry 34*, 2163−2171.
20. Stankovich, M. T., and Soltysik, S. (1987) *Biochemistry 26*, 2627−2632.
21. Nishina, Y., Sato, K., Shiga, K., Fujii, S., Kuroda, K., and Miura, R. (1992) *J. Biochem. (Tokyo) 111*, 699−706.
22. Nishina, Y., Sato, K., Hazekawa, I., and Shiga, K. (1995) *J. Biochem. (Tokyo) 117*, 800−808.
23. Pellett, J. D., Sabaj, K. M., Stephens, A. W., Bell, A. F., Wu, J., Tonge, P. J., and Stankovich, M. T. (2000) *Biochemistry 39*, 13982−13992.
24. Engel, P. C. (1992) in *Chemistry and Biochemistry of Flavoproteins* (Müller, F., Ed.) pp 597−655, CRC Press, Boca Raton, FL.
25. Kim, J.-J. P., Wang, M., and Paschke, R. (1993) *Proc. Natl. Acad. Sci. U.S.A. 90*, 7523−7527.
26. Matsubara, Y., Indo, Y., Naito, E., Ozasa, H., Glassberg, R., Vockley, J., Ikeda, Y., Kraus, J., and Tanaka, K. (1989) *J. Biol. Chem. 264*, 16321−16331.
27. Mancini-Samuelson, G. J. (1996) Ph.D. Thesis, University of Minnesota, Minneapolis, MN.
28. Sambrook, J., Fritsch, E. F., and Maniatis, T. (1989) in *Molecular Cloning; A Laboratory Manual* (Nolan, C., Ed.) 2nd ed., Cold Spring Harbor Laboratory Press, Cold Spring Harbor, NY.
29. Studier, F. W. (1991) *J. Mol. Biol. 219*, 37−34.
30. DuPlessis, E. R., Pellett, J. D., Stankovich, M. T., and Thorpe, C. (1998) *Biochemistry 37*, 10469−10477.
31. McIlwain, H. (1937) *J. Chem. Soc. 2*, 1704−1711.
32. Lehman, T. C., Hale, D. E., Bhala, A., and Thorpe, C. (1990) *Anal. Biochem. 186*, 280−284.
33. Williamson, G., and Engel, P. C. (1984) *Biochem. J. 218*, 521−529.
34. Munro, A. W., and Noble, M. A. (1999) *Methods Mol. Biol. 131*, 0000.
35. Stankovich, M. T. (1980) *Anal. Biochem. 109*, 295−308.
36. Stankovich, M. T., and Fox, B. (1983) *Biochemistry 22*, 4466−4472.
37. Einarsdötter, G. H., Stankovich, M. T., and Tu, S. C. (1988) *Biochemistry 27*, 3277−3285.
38. Saijo, T., and Tanaka, K. (1995) *J. Biol. Chem. 270*, 1899−1907.
39. Williamson, G., and Engel, P. C. (1982) *Biochim. Biophys. Acta 706*, 245−248.
40. Müller, F. (1992) in *Chemistry and Biochemistry of Flavoproteins* (Müller, F., Ed.) pp 1−71, CRC Press, Boca Raton, FL.
41. Edmonson, D., and Ghisla, S. (1999) *Methods Mol. Biol. 131*, 0000.
42. Hunter, C. A., and Sanders, J. K. M. (1990) *J. Am. Chem. Soc. 112*, 5525−5534.
43. Johnson, B. D., Mancini-Samuelson, G. J., and Stankovich, M. T. (1995) *Biochemistry 34*, 7047−7055.
44. Schopfer, L. M., Massey, V., Ghisla, S., and Thorpe, C. (1988) *Biochemistry 27*, 6599−6611.
45. Stadtman, E. R. (1957) *Methods Enzymol. 3*, 931−941.
46. Massey, V., and Ghisla, S. (1974) *Ann. N.Y. Acad. Sci. 227*, 446−465.
47. Thorpe, C., Matthews, R. G., and Williams, C., Jr. (1979) *Biochemistry 18*, 331−337.
48. Rudik, I., Ghisla, S., and Thorpe, C. (1998) *Biochemistry 37*, 8437−8445.
49. Rudik, I., Bell, A. F., Tonge, P. J., and Thorpe, C. (2000) *Biochemistry 39*, 92−101.
50. Miura, R., Nishina, Y., Fujii, S., and Shiga, K. (1996) *J. Biochem. (Tokyo) 119*, 512−519.
51. Tamaoki, H., Nishina, Shiga, K., and Miura, R. (1999) *J. Biochem. (Tokyo) 125*, 285−296.

BI010206S